

APPLICATION RESEARCH ON THE DUAL-SPOOL VALVE CONTROL SYSTEM IN A HYDRAULIC –FARM-ORIENTED LOAD TRACTOR

双阀芯液压控制系统在农用装载机中的应用研究

A.P. Wenhua Jia^{*1)}, Prof. Chenbo Yin²⁾, Dr. Binghui Jia¹⁾, Dr. Guo Li¹⁾, A.P. Dasheng Zhu¹⁾, Song Zhang³⁾

¹⁾ School of Mechanical Engineering, Nanjing Institute of Technology, Jiangsu / China;

²⁾ School of Mechanical and Power Engineering, Nanjing University of Technology, Jiangsu 211800 / China;

³⁾ IPEK – Institut für Produktentwicklung, Karlsruher Institut für Technologie (KIT), Karlsruhe / Germany

Tel: +13505177950; E-mail: geovrml@163.com

Keywords: Dual spool; Stress response; Power consumption; Farm-oriented load tractor

ABSTRACT

To cope with the increasingly severe working environment confronting agricultural load tractors, load tractor design must consider the comprehensive influences of noise immunity, control precision, and power loss, among others, of hydraulic systems. A SY235 load tractor and a dual-spool multi-way valve-based prototype were applied as research objects in this research. The antisymmetric data processing function of AMESIM software was employed to update and replenish point data, while a cubic interpolation method was adopted to process the data. In addition, the displacement characteristics, inlet and outlet pressures, and energy consumption of each cylinder in the hydraulic systems of both load tractors equipped respectively with the dual-spool multi-way valve and single-spool multi-way valve were investigated. Meanwhile, a single action experiment was performed on the booms, bucket rods, and buckets of the two load tractors. A comparison of the real test with the simulation model demonstrated that the cylinder controlled by the dual-spool valve exhibited small pressure and power consumption and quick displacement response. Therefore, the cylinders controlled by the dual-spool multi-way valve system had quicker pressure response, smaller pressure and overshoot, and superior overall manipulability. Finally, retraction and external swinging experiments of the buckets were performed on the dual-spool experimental prototype. Experimental results demonstrated that the dual-spool multi-way valve system exhibited faster displacement response and more superior overall performance compared with the single-spool control system. The simulation model combined with the real vehicle experiment is of great significance to the further study of the static and dynamic characteristics and energy-saving performance of the dual-spool agricultural load tractor.

摘要

为应对越来越恶劣的农用装载机工作环境，挖掘机设计需综合考虑液压系统的抗干扰性、控制精度、功率损失等的影响。论文以 SY235 型号装载机和双阀芯多路阀原型为依据，利用 AMESIM 的反对称数据处理功能更新补充点数据和三次方插值方法处理数据，研究了双阀芯多路阀和单阀芯多路阀装载机液压系统中各油缸的位移特性、进出口压力特性以及能耗情况。通过实车实验与仿真模型进行对比，结果表明双阀芯多路阀控制的油缸压力小，功率消耗小，在位移响应上也是双阀芯系统稍快。通过整机工况实验，得出了双阀芯多路阀控制系统的油缸压力响应较快，压力较小，超调量较小，整体操作性能占优，用双阀芯试验样机做铲斗内收和外摆实验，双阀芯控制系统在位移响应上比单阀芯控制系统快，双阀芯多路阀整体性能占优。仿真模型结合实车实验对深入研究双阀芯农用装载机的静动态特性和节能性能具有重要意义。

INTRODUCTION

Farm-oriented load tractors are widely used in the fields of basic construction, agricultural facilities, construction of new rural areas, and other aspects. These equipments are important in the basic construction of rural areas. Consequently, increased performance requirements of the hydraulic system of the load tractor are needed. The dual-spool system can independently control the inlet oil pressure and return oil pressure under the premise that all working conditions of executive mechanisms are satisfied. Various combinations of the ratio between two spool displacements, accompanied by sensor technology, can better deal with the matching relation between pressure and load, as well as realize the functions that traditional single-valve spool systems can not.

The performance of a hydraulic farm-oriented load tractor depends on whether the match among various subsystems is reasonable (Casoli Paolo, Anthony Alvin, 2013; Yi Yuan and Yu Tu, 2013; Choi Kyujeong et al, 2015; Kumar A, 2013). In recent years, researchers from many universities and institutions in China and abroad have conducted extensive research on the static and dynamic behaviours of the main

pump, the matching performances of engine power, and the orifice area of the throttling groove in the multiple directional control valve spool (Xiong Y et al, 2015; Barreto CEAG and Schiozer DJ, 2015; Lisowski E et al, 2014), and have gained numerous achievements. The concept of independent control was proposed by the German professor, Bark, in the control theory of cartridge valve in 1987 (Ye Y et al, 2014; Kumar A et al, 2013). Matti et al (2015) conducted an in-depth study on the principles of independent control, and then used multiple digital valves to replace traditional proportional valves to discuss the changes in system performance. Some researchers utilized multiple cartridge valves to replace traditional single-core valves and study the independent control strategy (Claudio Alimonti et al, 2010; Feng C and Kamat V.R., 2013). Feng used double-valve core systems to independently control the executive mechanisms, as well as study the dynamics and energy-saving features of the systems. They concluded that the system oil pressure and energy consumption were reduced by the use of double-valve core control technology, realizing nearly 15% in energy saving (Mattila J and Virvalo T., 2000). At CONEXPO Asia2007, American equipment manufacturers displayed a type of newly developed hydraulic load tractor. According to their data, this type of load tractor adopts independent control technology for load ports. Compared with traditional hydraulic load tractors, the newly developed hydraulic load tractors can reduce energy consumption by 25% and increase productivity by 10% (Atik FA et al, 2005; Falck Tillmann, 2012). In the VT02 series of Linde Corp., Germany, double-core multi-control valves are used and pressure compensators are preserved in valve cores. American EATON Corp.'s Ultratics Corp. provides a series of electro-hydraulic control solutions, including a double-core electro-hydraulic valve control system that adopts independent control technology for use in load tractors, loaders, and aerial vehicles and other agricultural machineries.

The remainder of this paper is organized as follows. Section 2 compares single-spool multi-control valves and dual-spool control technology. Section 3 analyzes the dual-spool multi-way valve farm-oriented load tractor hydraulic system characteristics. Section 4 analyzes the aforementioned system characteristics by adopting the method of combination simulation and experiment and comparing the single-core multi-way valve with the double-core multiplex valve. Section 5 summarizes the conclusions

MATERIAL AND METHOD

Mathematical Model of Dual-spool Valve-controlled Hydraulic Cylinder Systems

Compared with single-spool multi-control valves, dual-spool control technology is the combination of a number of technologies, such as electro-hydraulic proportional and sensor technology. Two valve cores are used in the main valve, and executive mechanisms are independently controlled by single-switching valves. The schematic structures of a single group of dual-spool valves are shown in Figures 1 and 2. The parameters of the vehicle operating device of this corresponding load tractor is shown in Table1.

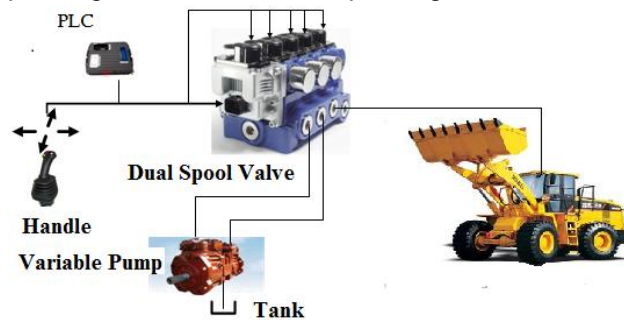


Fig.1 - Dual spool multi-way valve

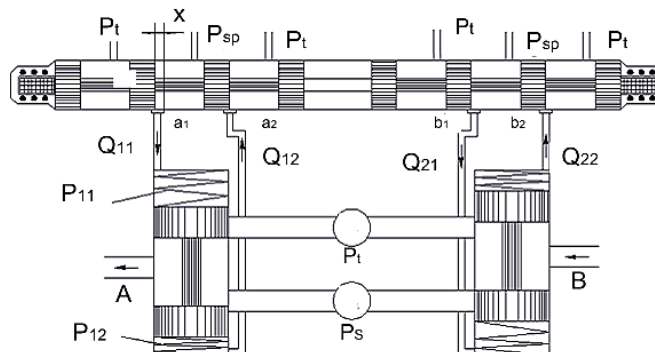


Fig.2 - Dual spool valve structure of an load tractor hydraulic system

Table 1

Parameters of the vehicle operating device	
Definition of the parameter	Parameter values
A. Maximum digging depth	3.03 m
B. The horizontal distance between the bucket and the center of the front wheel	5.31 m
C. The horizontal distance between the bucket and the rotating center	4.11 m
D. The horizontal distance between the bucket on top and the rotating center	2.64 m
E. Maximum digging height	3.40 m
F. Maximum unloading height	2.85 m

In Figure 2, P_s is main pressure, P_{sp} is pilot oil pressure, P_t is oil return pressure, A and B is working oil port, P_{11} and P_{12} are pressure at both ends of the valve. a_1, a_2, a_3 and a_4 are ports of pilot valve. $Q_{11}, Q_{12}, Q_{13},$ and Q_{14} are flow at each intersection.

The dual-spool valve is symmetric, and its throttle area gradients are equal. The optimal displacement relationship between the two spools is obtained by adjusting the displacement ratio of the two main spools in order to adapt to all kinds of working conditions. Their displacement relationship can also be flexibly adjusted according to different working conditions. Assuming the positive direction of the piston movement is the positive direction of the Y coordinate, only the positive direction is studied because of the similarity of theories.

The displacement ratio of valve spools 2 and 1 is provided as $x_1 / x_2 = m_1$. The cylinder area ratio of the rod and rodless chambers is $A_1 / A_2 = n$. Q_L is used as the load flow.

$$\begin{cases} P_L = F/A_1 = P_1 - nP_2 \\ Q_L = (Q_1 + nQ_2)/(1 + n^2) \end{cases} \quad (1)$$

Where P_L is load pressure, F is load equivalent effect, A_1 is area of rod chamber, A_2 is area of rodless chamber, P_1 is pressure of rod chamber, P_2 is pressure of rodless chamber.

The characteristic equation of the system pressure and flow is as follow.

$$Q_L = C_d w_1 x_1 m_1 \sqrt{2/(\rho(m_1^2 + n^3))(P_s - P_L)} \quad (2)$$

Where C_d is the flow coefficient, ρ is the oil density, and $w_1 = w_2$ is the throttling area gradient.

Flow gain of valve 1:

$$K_{qp1} = \partial Q_L / \partial x_1 = C_d w_1 m_1^3 / (m_1^2 + n^3) \sqrt{2/(\rho(m_1^2 + n^3))(P_s - P_L)} \quad (3)$$

Flow gain of valve 2:

$$K_{qp2} = \partial Q_L / \partial x_2 = C_d w_1 n^3 / (m_1^2 + n^3) \sqrt{2/(\rho(m_1^2 + n^3))(P_s - P_L)} \quad (4)$$

Flow gain of the dual-spool valve:

$$K_{qp} = K_{qp1} + K_{qp2} m_1 = C_d w_1 m_1 \sqrt{2/(\rho(m_1^2 + n^3))(P_s - P_L)} \quad (5)$$

Flow pressure coefficient:

$$K_{cp} = -\partial Q_L / \partial P_L = C_d w_1 x_1 m_1 \sqrt{2/(\rho(m_1^2 + n^3))(P_s - P_L)} / 2(P_s - P_L) \quad (6)$$

System linear equation of the pressure and flow characteristic:

$$Q_L = K_{qp} x_1 - K_{cp} P_L \quad (7)$$

Initial volume of the hydraulic cylinder is $V_{10} = V_{20} = (V_1 + V_2) / 2 = V_0$, and Y is infinitesimal.

Flow continuity equation of the rodless chamber:

$$Q_1 = A_1 dY/dt + V_0/\beta_e \cdot dP_1/dt + (C_{ec} + C_{ic})P_1 - C_{ic}P_2 \tag{8}$$

Flow continuity equation of the rod chamber:

$$Q_2 = A_2 dY/dt - V_0/\beta_e \cdot dP_2/dt - (C_{ec} + C_{ic})P_1 + C_{ic}P_2 \tag{9}$$

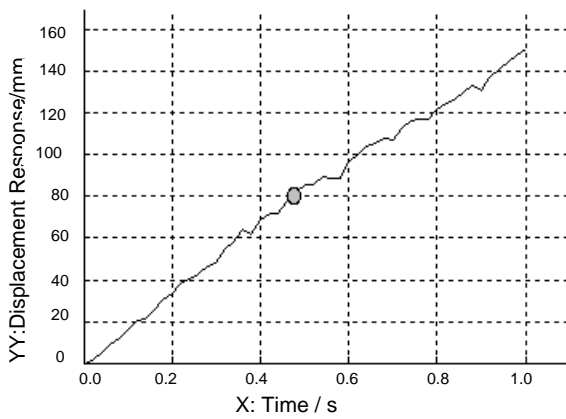
Where V_1 and rodless V_2 are the volumes of the rodless and rod cylinder chambers respectively, β_e is the elastic modulus of the hydraulic oil, C_{ec} is the external leakage coefficient, and C_{ic} is the internal leakage coefficient. C_{ic} , C_{ic1} are calculating coefficient.

Equation (10) can be obtained by solving the preceding equations:

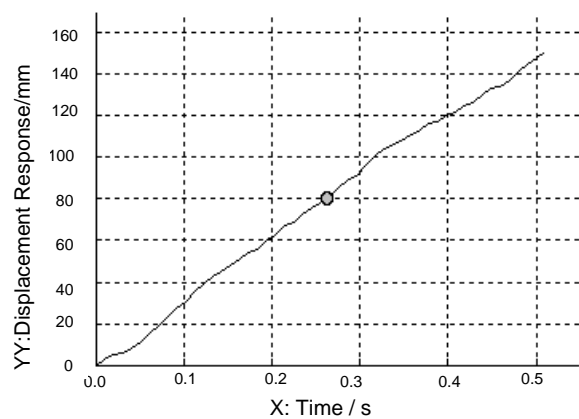
$$Q_L = A_1 dY/dt + V_1 + V_2/2(1+n^2)\beta_e \cdot dP_L/dt + C_{ic}P_L + C_{ic1}P_S \tag{10}$$

$$C_{ic} = \frac{m_1^2 + n^3}{(1+n^2)(m_1^2 + n^3)} C_{ec} + \frac{(1+n)(m_1^2 + n^2)}{(1+n^2)(m_1^2 + n^3)} C_{ic} \tag{11}$$

$$C_{ic1} = \frac{(1+n)(n^3 - n^2)}{(1+n^2)(m_1^2 + n^3)} C_{ic} \tag{12}$$



(a) $m_1 = 0.01$



(b) $m_1 = 100$

Fig.3 - Cylinder displacement response curve with different m_1

The parameters of the Model SY235 load tractor manufactured are adopted. The effective area ratio between the rod and rodless chambers of the bucket cylinder is $n=0.49$. The cases where m_1 equals 0.01, 0.49, 1, and 100 are studied. The experimental results are shown in Tables 2.

Table 2

Simulation schedule of cylinder displacement response				
Definition of the parameter	Parameter values			
m_1	0.01	0.49	1	100
T_1	0.47	0.37	0.31	0.27

Note: T_1 is the response time of different cases, and m_1 is the bucket cylinder displacement at 80 mm.

The displacement response time of the bucket cylinder decreases with the increase of m_1 , because if m_1 increases, the opening amount of the cylinder oil outlet will increase, thus reducing the back pressure and resistance.

Therefore, a large m_1 affects pressure response, whereas a small m_1 affects displacement response. The figures and tables clearly show that the cylinder pressure and displacement responses are both relatively good when m_1 is approximately 0.49. Furthermore, 0.49 is exactly the effective area ratio between the rod chamber and the rodless chamber of the bucket cylinder, n . Therefore, when m_1 equals n , both the cylinder pressure response and displacement response are relatively good.

Working Device Model

To model the machine ADAMS and perform a combined study and verification from Fig.5, the Model AMESim is established, constituting of the farm-oriented load tractor main pump, dual spool multi-control valves, executive mechanisms, and so on.

The rotary conditions of the load tractor are temporarily not studied. The slewing platform, chassis, and track are viewed as a whole. The operation can be obtained by Boolean operation. The model contains 15 components, as shown in Fig.4. Translational joint motion is added in the mobile assistant of the boom, arm, and bucket cylinder.

The excavation trace curve of the bucket prong is obtained. The maximum excavation height and depth are 9616 and 6739 mm respectively. Although these values are slightly different from the sample values of 9640 and 6785 mm, they are basically consistent, which demonstrates that the established model is correct

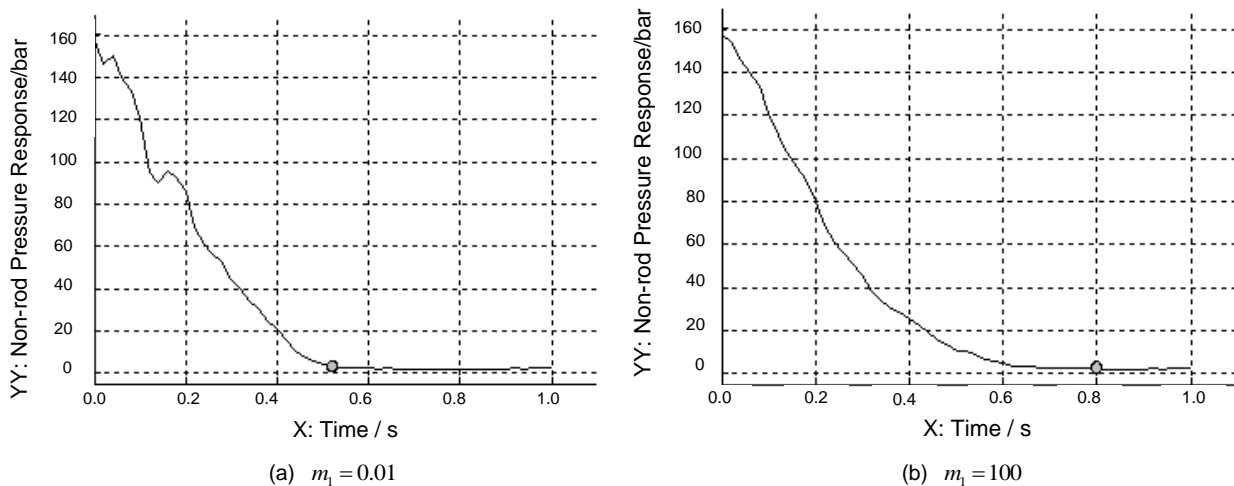


Fig.4 - Cylinder rodless chamber pressure response curve with different m_1

RESULTS

Distribution of heavy metal contents in vegetable field soils

The AMESIM model is established. The input speed of the engine is 2050 r/min, input power is 110 kW, and input torque is 512 N.M. Table 3 lists the main parameters of the hydraulic cylinder of load tractor.

Table 3

Main parameters of the farm-oriented load tractor

Hydraulic Cylinder		Diameter (mm)		Displacement (mm)
Boom	Piston	130		1332
	Rod Piston	90		
Bucket	Piston	120		1048
	Rod Piston	85		
Arm	Piston	135		1663
	Rod Piston	95		
Other	Whole (23,034 kg)	On-board platform	Gravity: 5705.48 kg, Density: 8278 kg/m ³	
		Off platform	Gravity: 17,294.52 kg, Density: 1548 kg/m ³	

The co-simulation mode is adopted for the joint simulation module, which is shown in the table 3. Table 3 clearly shows that the ratio between the displacements of two valve cores is 2.02, which can be transformed into the spring setting of two main spools.

The spring coefficients of main valves 1 and 2 are set to $k_1=9.55$ N/mm and $k_2=19.3$ N/mm respectively. The flow area and displacement relation of the main spool and the pilot spool are shown in Figs. 6(a) and (b) respectively.

Figure 7 shows the cylinder pressure and displacement characteristic curve of the simulated working conditions of the load tractor bucket adduction action. To facilitate analysis, the pressure characteristic curve covers the 0th to 15th second, and the displacement covers the 15th to 25th second. When the fuel tank just extends out, the pressure of the rod chamber and rodless chamber dramatically increases. This increase is attributed to the opening amount of the valve, which is relatively small at first, and the impact

on the rod chamber. Therefore, the pressure of the rod chamber is significantly increased. With the constant inflow of pilot signals, the opening amount of the valve core reaches the maximum, and the pressure of two chambers decreases. However, Figure 7 clearly shows that within 15 seconds, the pressure of the rod chamber of the bucket cylinder is basically larger than that of the rodless chamber. This difference is related to the initial state of the load tractor set in the simulation. The gravity of buckets is always downward because the load tractor equipment is just lifted to a suitable height in the simulation setting. Based on the equation $P_1A_1+f=P_2A_2$, the area of rodless chamber A_1 is larger than that of rod chamber A_2 . f represents the downward component of gravity. Therefore, the pressure of the rod chamber is large, and the displacement curve finally reaches 1048 mm. The whole process is consistent with the real working conditions of the farm-oriented load tractor prototype in agricultural production.

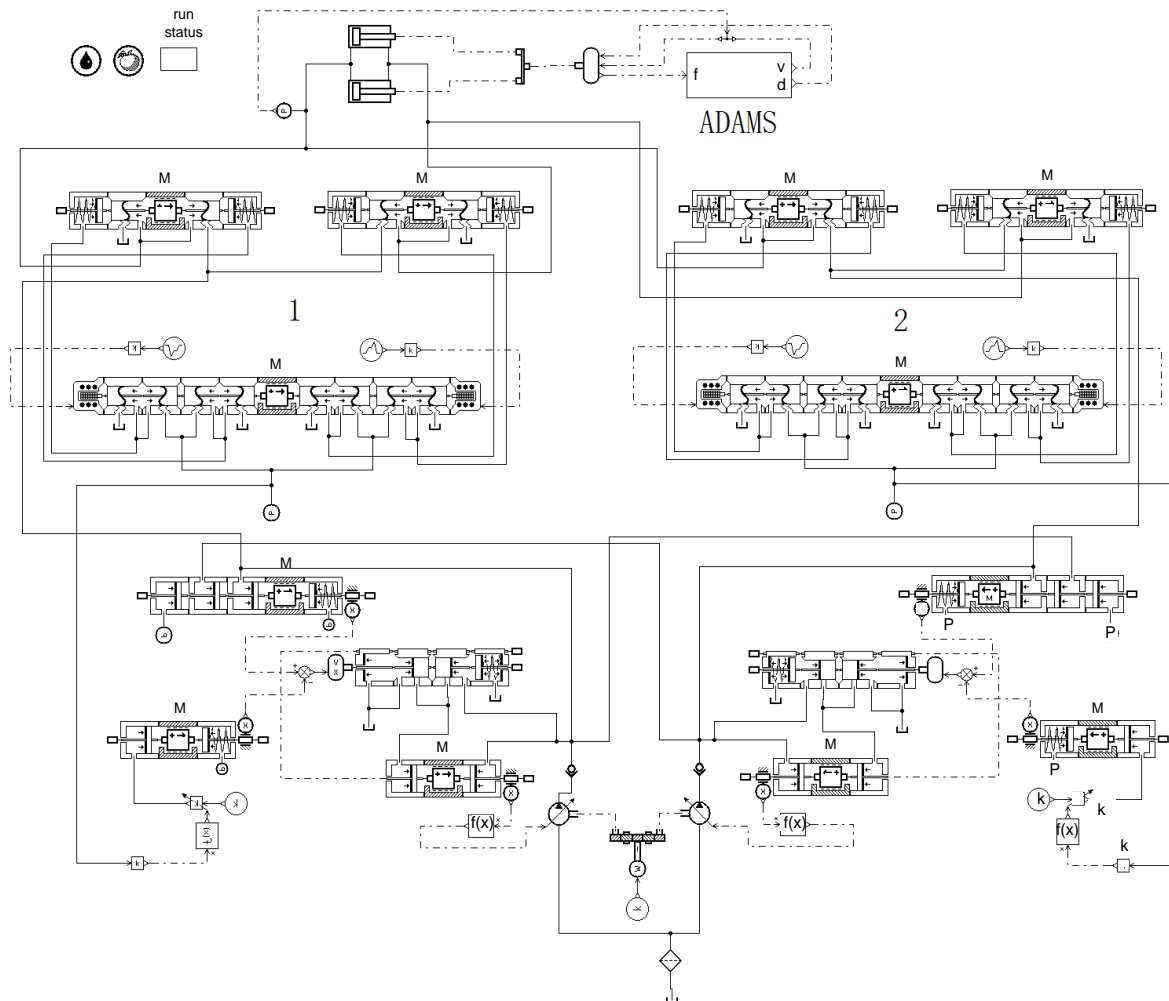


Fig. 5- Dual spool bucket joint AMESIM and ADAMS model simulation

In terms of the pressure of the cylinder rod chamber, and compared with the spool bucket circuit, the curve of dual spool valves varies faster than that of the single spool. At around the 13th second, the left and right cores become stable, faster than the single core. The average pressure of dual spool simulation is smaller than that of single core at 14 bar. In terms of cylinder rodless chamber pressure, the average curve of dual spool is smaller than that of the single core at 1.27 bar, with a maximum pressure difference of 4.1 bar. At around the 11th second, a small fluctuation occurs in the single core, whereas the dual spool remain smooth. At the 13th second, the dual spool reach a stable state, faster than the single core. In terms of displacement response, the dual spool are 2 seconds faster than the single core. In the aspect of energy consumption, both inlet oil pressure and return oil pressure are smaller than the single core. The following results can be obtained by using $P=pq$ and $q=vA$ to compute. The working power consumption of the load tractor stick with double-core multi-control valves within 15 seconds is 24.64 kW, while that for single-core multi-control valves is 30.61 kW. These values indicate that the single-core multi-control valve control system consumes more energy than the dual spool.

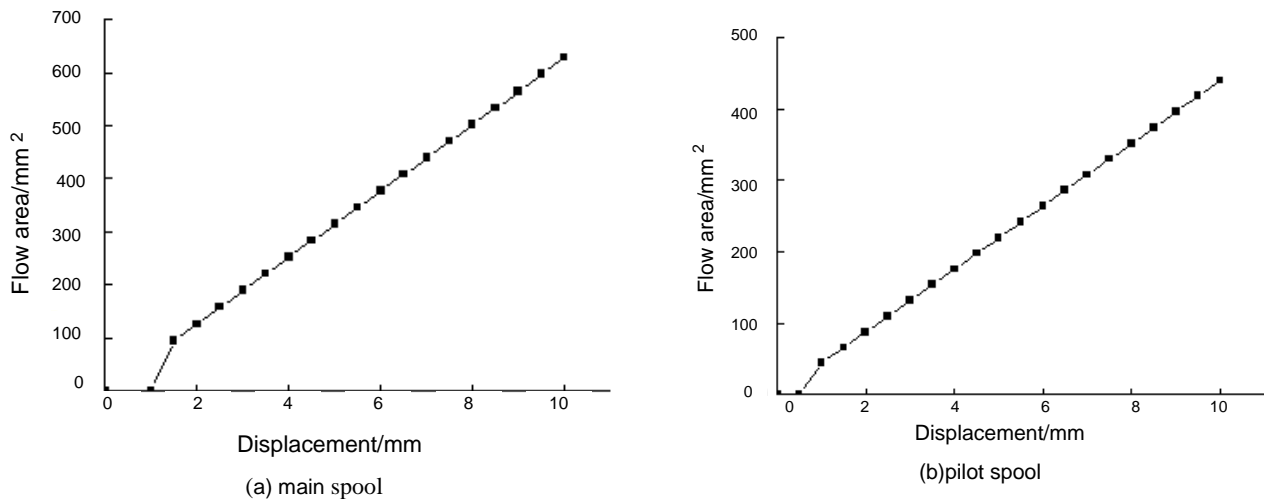


Fig. 6 - Relation graph between flow area and spool displacement

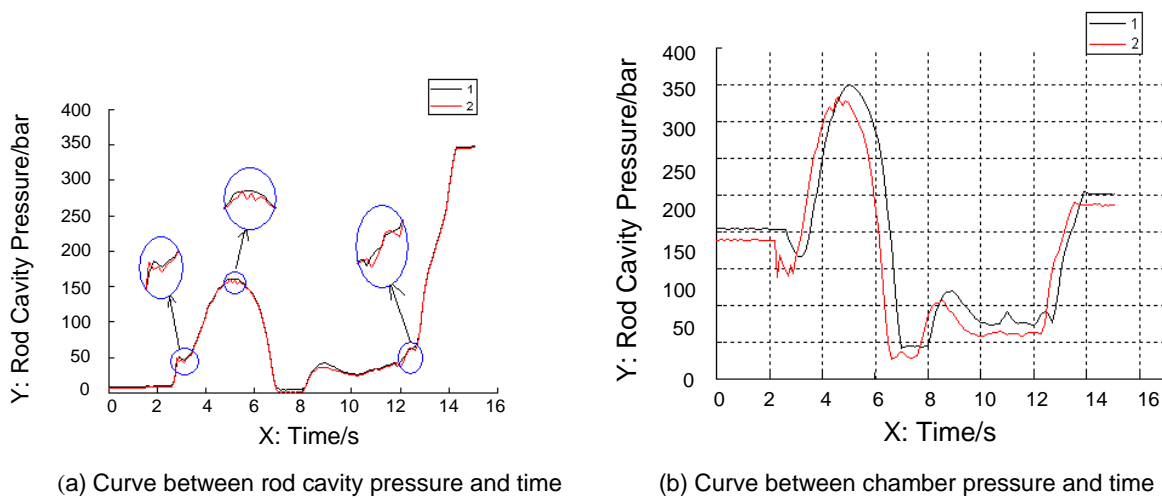


Fig.7 - Curve between pressure and time

Experiments for this Farm-oriented Load tractor Prototypes with Dual-spool Multi-control Valve

A bucket circuit is used for verification. The load tractor handle is operated to perform bucket adduction and outward swing action. The bucket cylinder pressure and displacement curve are obtained, as shown in Figure 8.

A comparison of the first 9 seconds in Fig. 8 with those in Fig. 7 indicates that the general trend is that the pressure in simulation is smaller than that in experiments. The average of the rodless chamber is smaller than 2.3 bar, while the rod chamber is smaller than 20 bar. The displacement speed of the simulated cylinder is faster than that in experiments because the practical factors consistent with real situations are not considered in the simulation, such as leakage and resistance along the way. At the beginning, actions have not started and the engine is idling. The curves for simulation and experiments correspond to relatively small values and vary slow. At the moment of valve opening, the pressure of the two chambers will suddenly increase, which can be seen from the two pressure curves of the rodless chamber. This increase happens twice in the experiment curves because when the load tractor is operated, the handle will jitter, a factor that is not excluded in simulation. The two pressure curves of the rod chamber reveal that a sudden pressure change occurs. Moreover, overflow happens owing to the effect of impact, and the pressure reaches the maximum. With the increase in opening amount of the valve core, the pressure of the two chambers constantly decreases. Before the bucket extends to the maximum length, the pressure of the rodless chamber is also smaller than that of the rod chamber, which is the same as in the simulation. Clearly, the joint simulation of the established double-core system satisfies the requirements method.

Experimental Comparison of Dual-spool and Single-spool Multi-control Load tractors

The same operations on dual-spool and single-spool load tractors are performed, including boom

lifting / lowering working conditions, arm adduction / outward swing working conditions, and bucket adduction / outward swing working conditions. The synchronization of the pilot handle is guaranteed. After handle operation, data are displayed in the PC software in real time. Fig. 9 shows the load tractor test site. The experimental data of the double-valve core and single-valve core load tractors are shown in Table 4.

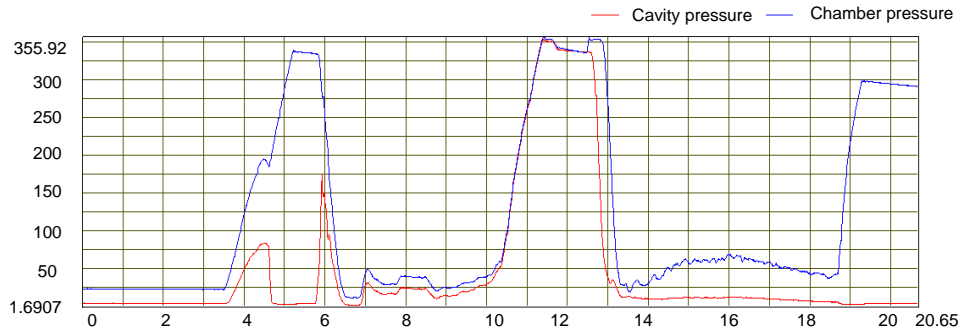


Fig. 8- Bucket cylinder pressure and displacement experiment curve

The data clearly show that the pressure of the double-core multi-control valve on the cylinder reaches the peak and stability faster than that of the single-core multi-control valve. The response of the double-core multi-control valve is faster. The pressure of the double-core multi-control valve on the cylinder is smaller, and the energy consumed within the same time interval is lower. The overshoot of the double-core multi-control valve is also lower than that of the single-core multi-control valve, which is another reason why the former reaches stable status faster. Moreover, due to the operation, overshoot fluctuates. As shown in the table, the pressure overshoot surpasses 100% in the cylinder rodless chamber of the bucket adduction working conditions and the rod chamber of the arm outward swing. This outcome indicates that the handle shakes in the two operations, thus causing shocks. Other working conditions are relatively smooth.



Fig.9 - Load tractor test site

Table 4

Farm-oriented load tractor experimental data of the dual-spool and single-spool valve (boom lift, varm adduction, bucket adduction)

Working conditions	Device		p_m /bar	p_w /bar	t_z /s	t_m /s	t_o /s	M_p /%
Boom lift	Chamber	Dual	118.758	117.2	50.22	1.01	7.9	2.6
		Singl	125.538	120.8	52.99	2.06	10.9	4.8
	Cavity	Dual	4.600	3.68	50.31	14.97	29.44	10.23
		Singl	6.632	5.45	53.41	17.85	32.86	11.98
Arm adduction	Chamber	Dual	124.58	80.081	10.50	5.74	7.92	54.9
		Singl	148.02	95.841	10.95	6.81	9.64	55.39
	Cavity	Dual	44.006	28.00	10.04	6.00	7.20	51.26
		Singl	46.546	31.83	10.91	6.57	8.73	55.4
Bucket adduction	Chamber	Dual	33	14.342	4.45	9.88	3.98	116.5
		Singl	35.1	15.742	7.74	1.37	5.31	123.7
	Cavity	Dual	48.795	28.2	4.05	1.06	1.49	66.9
		Singl	69.315	41.6	7.85	1.35	3.68	68.4

Note: The engine speed is 2050 r/min, p_m is the maximum pressure of the device in a corresponding working condition, p_w is the stable pressure of the device in a corresponding working condition, t_z is the time needed to complete the working condition, t_m is the time needed to reach the peak value of pressure, t_0 is the time needed to reach the stable pressure, and M_p is the overshoot. Rodless chamber refers to the rodless chamber of the cylinder, and rod chamber refers to the rod chamber of the cylinder.

CONCLUSIONS

The SY235 farm-oriented load tractor and a dual-spool multi-way valve-based prototype were applied for support. The electronic control improvements of the load tractor were completed. Oil capacity, power consumption, and displacement response capability of the dual-spool system were obtained. In addition, the performance of a single-spool system was comparative analyzed. The conclusions are shown as follows::

- Theories of double-core multi-control valves are analyzed. The conclusion drawn is that when the ratio between the displacements of the two valve cores in a double-core multi-control valve equals the ratio between the effective areas of hydraulic cylinder chambers, the pressure and displacement responses of the cylinder are relatively good.
- The experiments of bucket adduction and outward swing are carried out for a double-core load tractor prototype. The curves of experiment and simulation are compared and analyzed to verify that the joint simulation model of the double-core system is correct.
- The same single actions of boom, arm, and bucket are tested for two load tractors. The double-core control system is fast in pressure response and has more fluctuations at the beginning of actions, which is not very stable. The dual-spool control system reaches stable status first. The average pressure of the double-core multi-control cylinder is lower than that of the single-core system, which has low energy consumption. The double-core control system is faster than the single-core control system in displacement response. The overall performance of the double-core multi-control valves is better than the single ones. The SY235C-8S prototype can provide the test platform for further improvement of dual-spool multi-control valves.

Through the simulation research and prototype experiment, the power consumption of the dual-spool valve is found to be smaller and more energy saving in a farm-oriented load tractor. The study also found that the system has a certain internal leakage, which is the direction of further research for early rollover warning design in agricultural production.

ACKNOWLEDGEMENT

This work was supported in part by The National Natural Science Fund of China, Jiangsu Natural Science Foundation, University of Jiangsu Natural Science Foundation, and SANY Co., Ltd. in Jiangsu. Lecturer, Support Fund Nos. 51505211, 51505212, 51405222, 11302097, and BK20130741.

REFERENCES

- [1] Casoli P., Anthony A., (2013), Gray box modeling of an excavator's variable displacement hydraulic pump for fast simulation of excavation cycles, *Control Engineering Practice*, Pergamon Press, Vol.21, Issue 5, pp.483-494, New York/U.S.A;
- [2] Yi Yuan, Yu Tu, (2013), The Load Sensing Principle of Proportion Multi-channel Valve and its Application in Excavator, *2013-Third International Conference on Intelligent System Design & Engineering Applications*, Vol.1, pp.1469-1472, Brown University Psychopharmacology Update/Hong Kong;
- [3] Choi Kyujeong, Seo Jaho, Nam Yongyun, Kim Kyeong Uk, (2015), Energy-saving in excavators with application of independent metering valve, *Journal of Mechanical Science and Technology*, Vol.29, Issue 1, pp.387-395 Korean Society of Mechanical Engineers, Seoul / Korean;
- [4] Kumar A., Fitzsimons B., Trombetta C., (2013), Atrioventricular Groove Hematoma During Mitral Valve/Tricuspid Valve Repair: Transesophageal Echocardiography Characteristics, *Anesthesia and analgesia*, Vol.115, Issue 5, pp.986-988 International Anesthesia Research Society, New York / U.S.A;
- [5] Xiong Y, Wei J.H, Feng R.L., (2015), Adaptive robust control of a high-response dual proportional solenoid valve with flow force compensation, *Proceedings of the institution of mechanical engineers part I-Journal of systems and control engineering*, Vol. 229, Issue.1, pp.3-26, University of Bath/UK;
- [6] Barreto C., Schiozer D.J. (2015), Optimal placement design of inflow control valve using a dynamic

- optimization process based on technical and economic indicators, *Journal of petroleum science and engineering*, Vol.125, Issue.1, pp.117-127, Elsevier Science BV, Amsterdam/Netherlands;
- [7] Lisowski E., Czyzycki W., Rajda J., (2014), Multifunctional four-port directional control valve constructed from logic valves, *Energy conversion and management*, Vol.87, Issue 10, pp.905-913, Pergamon Elsevier Science LTD , Oxford/England;
- [8] Ye Y, Yin C.B., Li X.D., Zhou W.J., Yuan F.F., (2014), Effects of groove shape of notch on the flow characteristics of spool valve, *Energy conversion and management*, Vol.86, Issue 10, pp.1091-1101, Pergamon Elsevier Science LTD , Oxford/England;
- [9] Kumar A., Fitzsimons B., Trombetta C., (2013), Atrioventricular Groove Hematoma During Mitral Valve/Tricuspid Valve Repair: Transesophageal Echocardiography Characteristics, *Anesthesia and analgesia*, Vol.116, Issue 5, pp.986-988, Cleveland, International Anesthesia Research Society, New York/U.S.A;
- [10] Claudio Alimonti, Gioia Falcone, Oladele Bello, (2010), Two-phase flow characteristics in multiple orifice valves, *Experimental Thermal and Fluid Science*, Vol.34, Issue.8, pp.1324-1333, Elsevier Science INC, York/U.S.A;
- [11] Feng C; Kamat V.R., (2013), Plane registration leveraged by global constraints for context-aware AEC applications, *Computer-Aided Civil and Infrastructure Engineering*, Vol.28, Issue.5, pp.325–343 Blackwell Publishers, Inc, Malden/U.S.A;
- [12] Matti Linjama, Matti Vilenius, (2005), Improved digital hydraulic tracking control of water hydraulic cylinder drive, *International Journal of Fluid Power*, Vol.6, Issue 1, pp.29-39, TuTech Innovation, West Lafayette/U.S.A;
- [13] Mattila J, Virvalo T., (2000), Energy-efficient motion control of a hydraulic manipulator, *Proceedings 2000 ICRA, IEEE International Conference on Robotics and Automation*, Piscataway, Vol.24-28, pp.3000-3006, NJ/USA;
- [14] Atik FA., Pettersson G.B., Sigurdsson G., Gonzalez-Stawinski G.V., Sabik E.M., Kim A., Svensson, L.G., (2005), The ultimate development of mitral valve endocarditis: Atrioventricular separation, atrioventricular groove abscess and hemorrhagic pericarditis, *Journal of heart valve disease*, Vol.14, Issue 1, pp.29-32, Icr Publishers, Pinner/England;
- [15] Falck Tillmann., Dreesen Philippe., De Brabanter Kris, (2012), Least-Squares Support Vector Machines for the identification of Wiener-Hammerstein systems. *Control Engineering Practice*, Vol.20, Issue 11, pp.1165-1174, New York/U.S.A, Pergamon Press.